International Journal of Advances in Engineering and Management (IJAEM)
Volume 3, Issue 2, pp: 108-129www.ijaem.net ISSN: 2395-5252

Partially Prestressed Concrete Members in Theoretical and Experimental Study

Vanda Trivana[*#1], Nakhelin Chhun[#1], Gerry Gerald Alexander[2]
[1]College of Civil Engineering, Tongji University, Shanghai,200092,China
[2]Department of Hydraulic and Ocean Engineering, National Cheng Kung University, 70101, Tainan, Taiwan

Corresponding Author: Vanda Trivana

Date of Submission: 15-01-2021 Revised:03-02-2021 Date of Acceptance: 18-02-2021

ABSTRACT: In the current design practice, there is a clear tendency to use partially prestressed beams because the concrete is allowed to have bending tensile stress and even crack during the load phase or occasional overload. If cracks occur, they are usually relatively small and evenly distributed, and when the load generated by the cracks is unloaded, the cracks can usually be completely closed. In addition, partially prestressed structures only require a small pretensioning force, so the number of prestressed tendon anchors can be reduced. Generally, the flexural strength is either provided by prestressed steel bars and non-prestressed reinforced concrete, or is guaranteed by a sufficient number of high-strength steel bars that are stretched below the allowable value. Owing to the small pre-tensioning force value, the bottom flange size required to bear the compressive stress of the beam during the loading stage can be reduced or completely eliminated. This not only significantly simplifies the mold components, but also reduces mold costs and makes the structure more beautiful. In addition, due to the reduction of the tensile stress requirements in the concrete under load, the deflection characteristics of the beam can be significantly improved. The member can avoid the excessive camber in the unloaded stage, and for the specific load situation, the pretensioning force can be selected to obtain the required deflection. Partially prestressed concrete can be selected according to the function and environmental conditions of the structure, and different prestress values can be selected to control the deformation and cracks of the component in specific circumstance, and have sufficient ductility before failure. Therefore, it is predicted that partially prestressed concrete structures play vital role in promoting prestressed concrete structures.

KEYWORDS: PartiallyPrestressed Concrete,PretensioningForce,Crack,Deformation

I. INTRODUCTION

Partially prestressing as defined by the Joint ACI-ASCE Committee 423 is "An approach in design and construction in which prestressed reinforcement or a combination of prestressed and non-prestressed reinforcement is used such that tension and cracking in concrete due to flexure are allowed under service dad and live loads, while serviceability and strength requirements are satisfied." Due to the study of Bruggeling [1], for partially prestressed concrete structures, the degree of prestress, κ, is the ratio of the applied partial prestressing force, P_{part}, and the prestressing force, P_{full}, which caused full prestress under maximum load, i.e., zero stress at the extreme fiber of concrete member:

$$\kappa = \frac{P_{part}}{P_{full}}$$

The above formula can be used only when both prestressed forces have the same centroid. When fewer tendons are used in partial prestressing, then κ becomes:

$$\kappa = \frac{M_{Dec}}{M_{max}}$$

Where

M_{Dec} : moment which produces zero concrete stress at the extreme fiber of a section (nearest to the centroid of the prestressing force), when added to the action of the effective press alone,

M_{max} : maximum moment caused by the total service load (dead load plus live load).

II. PRACTICAL APPROACH OF PARTICALLY PRESTRESSED CONCRETE IN SLAB

PARTICAL PRESTRESSED CONCRETE SLAB AS AN ALTERNATIVE FOR VEHICL DECKS OF STEEL TRUSS BRIDGES

International Journal of Advances in Engineering and Management (IJAEM)
Volume 3, Issue 2, pp: 108-129www.ijaem.net ISSN: 2395-5252

According to Sutarja et al. [2], relative experiments on the partially prestressed concrete of alternative vehicle slab were made. Two concrete slab specimens were cast with 7000 mm length, 1000 mm width and 250 mm height. Symmetrical reinforcement consists of four non-prestressed steel bars and three strands, placed on the top and bottom of the slab. The result shows that under design load, the design moment was 27.43% less than the predicted cracking moment, which meant no crack occurred; under maximum load, cracks occurred evenly. Hence, it can be concluded that the partial prestressed concrete segmental slab was a good choice for vehicle decks of steel truss bridge.

STATIC BEHAVIOUR OF RC DECK SLABS PARTIALLY PRESTRESSED WITH HYBRID REINFORCED POLYMER TENDONS

The following is the study of Static behavior of RC deck slabs partially prestressed with hybrid reinforced polymer tendons from Wang et al. [3]. Three types of reinforcements were used in the experiment of RC deck slabs: steel, glass FRP (GFRP) and basalt/carbon (B/C) hybrid FRP bars. Seven RC full-scale deck slabs were prepared for the experiment. The slabs were square in plane with the length of 2400 mm and thickness of 200 mm. Five slabs were partially prestressed with B/C hybrid FRP tendons; other two slabs were non-prestressed working control slabs. The reinforcements of the non-prestressed slabs were designed according to the empirical design method of CSA. The prestressed FRP-RC deck slabs were designed according to three parameters: the FRP-reduction factor (RF=reduction in the FRP transverse reinforcement area with respect to the FRP-RC control slab), the prestressing level (P% = the ratio of prestress force to tensile capacity, in percentage), and the partial prestressing index (PPI = ratio of the prestressed FRP reinforcement to the total FRP reinforcement in the transverse direction of the slab). All tested specimens were tested under concentrate load with using two-actuator loading machine.

The control slab reinforced with steel bar (SS) failed in flexural/punching mode after yielding of steel bars, and larger numbers of cracks were observed with smaller spacing. The non-prestressed FRP-RC control slabs failed in punching failure mode. Prestressed and non-prestressed FRP-RC slabs showed no obvious differences in cracks. Prestressed FRP-RC slabs also failed in punching failure mode, except for SF0.29P50-0.5 slab, which failed in flexural/punching mode. This failure may be caused of the relatively low-concrete strength in the slab. Fig. 1 shows the failure modes of corresponding slabs. The testing results show that the prestressing level, partial prestressing index and FRP-reduction factor can be neglected in the failure mode of the prestressed FRP-RC slabs.

Fig.1. Crack pattern of (a) SS (b) SF and (c) SF0.37P35-0.5 slab

Due to the results, it can be seen that SF slabs had 35% lower than SS slab in cracking load due to the difference of reinforcement distribution along the slabs, and bonding characteristics of FRP and steel reinforcements. The cracking load in FRP-RC were 15-26% higher than in SF. The effect of prestressing level on cracking load is more significant than the FRP-reduction factor. The failure load of non-prestressed FRP-RC slabs is three times higher than design factored load (208.25 kN) due to high strength of FRP reinforcement. The failure load of prestressed FRP-RC are 2.6-3.4 times higher than the design factored load.

Load and maximum crack width relations is shown in Fig. 2. The results indicate that the amount of FRP reinforcement can be reduced and crack width can be guaranteed by using a proper method for design. Moreover, according to the results, FRP-reduction factor and prestressing level have significant effects on crack width, while the partial prestressing index can be neglected here.

Due to the results, it can be seen that SF slabs had 35% lower than SS slab in cracking load due to the difference of reinforcement distribution along the slabs, and bonding characteristics of FRP and steel reinforcements. The cracking load in FRP-

International Journal of Advances in Engineering and Management (IJAEM)
Volume 3, Issue 2, pp: 108-129www.ijaem.net ISSN: 2395-5252

RC were 15-26% higher than in SF. The effect of prestressing level on cracking load is more significant than the FRP-reduction factor. The failure load of non-prestressed FRP-RC slabs is three times higher than design factored load (208.25 kN) due to high strength of FRP reinforcement. The failure load of prestressed FRP-RC are 2.6-3.4 times higher than the design factored load.

Load and maximum crack width relations is shown in Fig. 2. The results indicate that the amount of FRP reinforcement can be reduced and crack width can be guaranteed by using a proper method for design. Moreover, according to the results, FRP-reduction factor and prestressing level have significant effects on crack width, while the partial prestressing index can be neglected here.

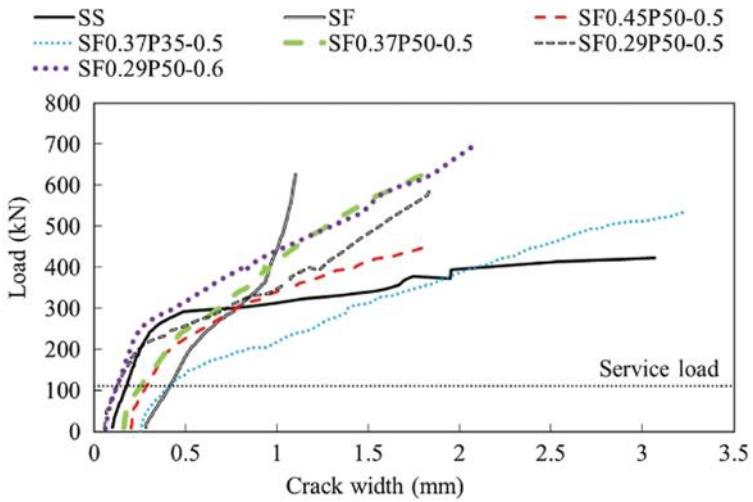

Fig. 2. Load-maximum crack widths curves

Fig.3 shows load-maximum deflection curves of all slab specimens. The first part up to cracking load exhibits the behavior of un-cracked slab with the gross inertia of the concrete cross section and the second, while the second part represents the cracked slab with reduced inertia. The load-deflection curve was linear up to cracking load (131 kN), and then turned to non-linear up to failure due to the cracking of concrete and yielding of steel reinforcement. SF0.29P50-0.6 had the highest post-cracking stiffness, where SF0.37P35-0.5 had the lowest. Post-cracking stiffness increases by increasing reinforcement area or prestressing level.

It can be seen that FRP-reduction factor and partial prestressing index have no effects on the deflection at service load. The maximum deflection of the slabs at the end of unloading stage is defined as residual deflection. Fig. 4 shows the residual deflection of the slabs. Steel-RC deck slab had small residual deflection compared to FRP-RC deck slab. However, part of prestressed slabs showed even smaller residual deflections than SS slab. The results show by increasing prestressing level, the residual deflection decreases. Fig. 5 shows deflection profiles alone half of transverse and longitudinal directions. In general, initially flat slab deformed into shallow cone outside the loaded area region.

International Journal of Advances in Engineering and Management (IJAEM)
Volume 3, Issue 2, pp: 108-129www.ijaem.net ISSN: 2395-5252

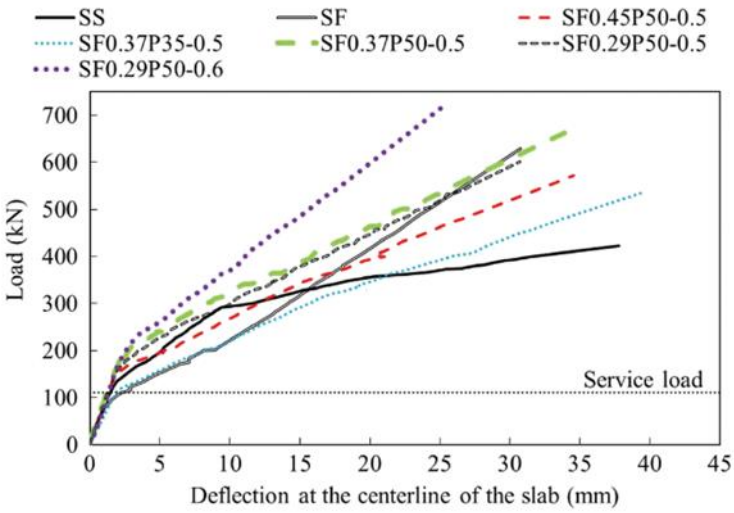

Fig.3. Load-maximum deflection curves

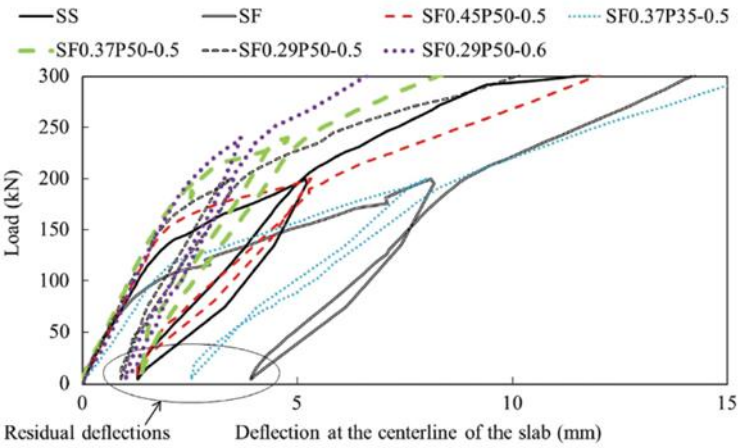

Fig.4. Load-maximum deflection curves including the unloading stages

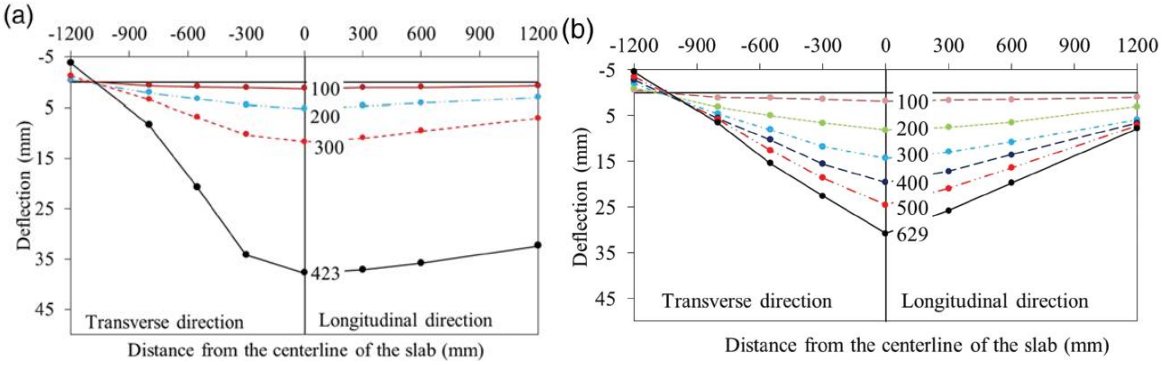

International Journal of Advances in Engineering and Management (IJAEM)
Volume 3, Issue 2, pp: 108-129www.ijaem.net ISSN: 2395-5252

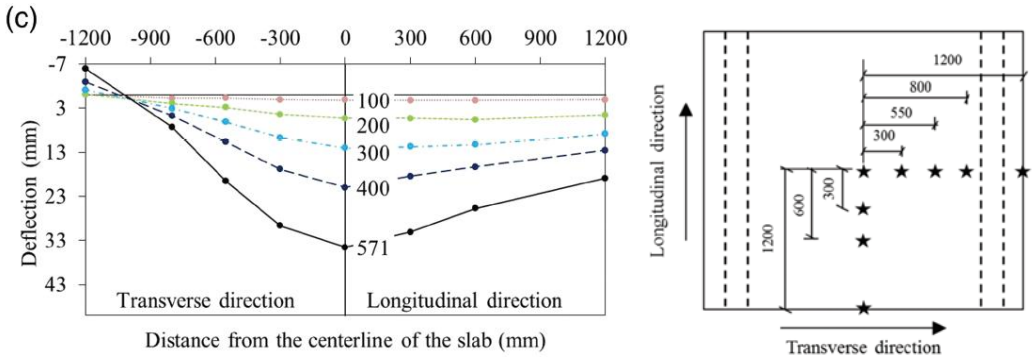

Fig.5. Deflection profiles along half of the transverse and longitudinal directions (a) SS (b) SF (c) SF0.45P50-0.5

The maximum measured strains of steel and FRP reinforcement of control slab were 13% of steel yield stain and 5% of FRP ultimate stain respectively at service level. The maximum reinforcement strain of SS slab was larger than its yielding stain, while the maximum strain of FRP reinforcement of FRP-RC slab was only 46% of its ultimate strain. The strains of non-prestressed reinforcement in prestressed FRP-RC slab were negligible at service level. These showed the fragmentation of non-prestressed bar due to shear stressed rather than tensile stresses. By increasing prestressing level or decreasing FRP-reduction factor, the stains in non-prestressed bar decreased. Concrete strains at service level were less than 6.4% of its ultimate strain, and 66%-88% of ultimate strain at failure level. By increasing prestressing level, it can be decreased strains of non-prestressed bars and residual strains. Fig. 5 demonstrates that by decreasing FRP-reduction factor, the strains of non-prestressed bars decreased.

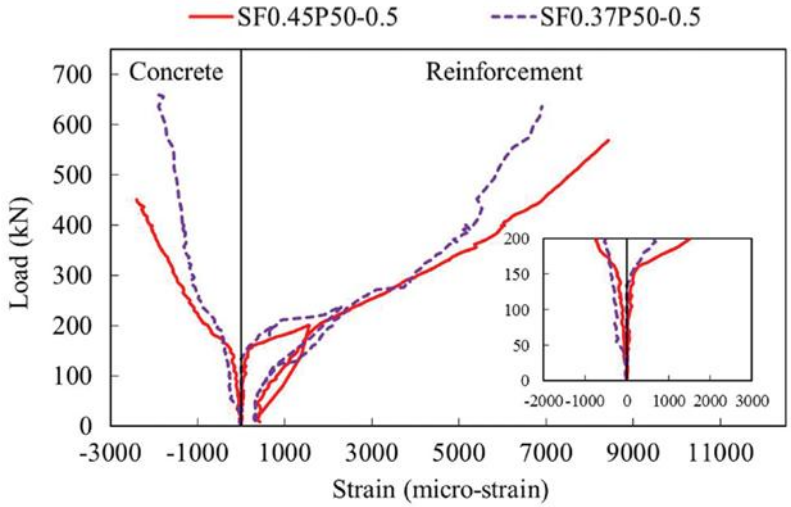

Fig.5. Effect of FRP-reduction factor on the strains of reinforcement and concrete

III. APPLICATION OF PARTICALLY PRESTRESSED CONCRETE IN BEAM

DEFLECTION OF UNBONDEDE PARTIALLY PRESTRESSED CONCRETE CONTINUOUS BEAMS

According to the study of Du et al.[4], the advantages of using unbonded tendons in prestressed concrete members are simple design, fast installation, easy to replace the defective one and economical design. Moment of inertia of cracked section I_{cr} is needed for determining the deflection of a unbonded partially prestressed concrete (UPPC) continuous beam after cracking. The main purpose of this research paper is to introduce the simplified method to estimate the value of I_{cr}.

The curve (Fig.6) resulted from experiment of UPPC beam shows three stages: elastic, cracked-elastic and plastic stage. The development from

International Journal of Advances in Engineering and Management (IJAEM)
Volume 3, Issue 2, pp: 108-129www.ijaem.net ISSN: 2395-5252

elastic to cracked-elastic is caused by the cracks at bottom of the beam. The development from cracked-elastic to plastic is caused by yielding of non-prestressed steel.

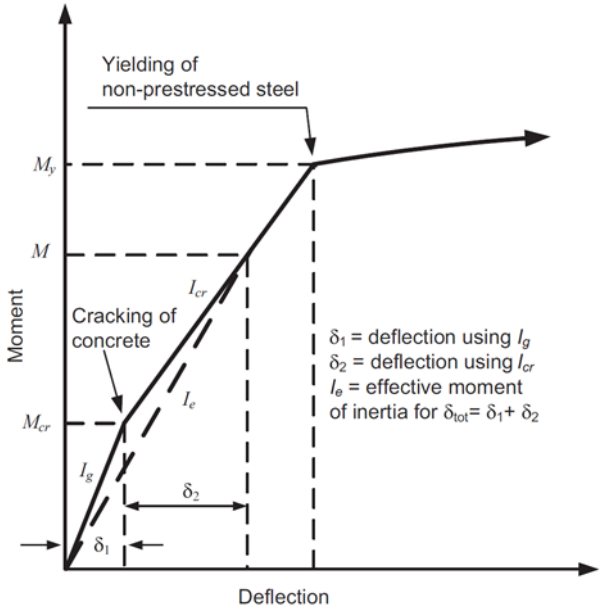

Fig.6. Moment-deflection curve of a UPPC beam

The deflection calculation depends on the section (cracked or uncracked). If the section is uncracked, then gross moment of inertia I_g can be used for the calculation of deflection. If the section is cracked, then using I_{cr} to calculate. The effective moment of inertia I_{cr} developed by Bransons:

$$I_e = \left(\frac{M_{cr}}{M}\right)^3 I_g + \left[1 - \left(\frac{M_{cr}}{M}\right)^3\right] I_{cr} \leq I_g$$

Where, M_{cr} and M are cracking and total applied moment at critical section respectively.

To calculate M_{cr}, two states of cracked sections are to be used: partially and fully cracked. Partially cracked referred to before yielding of non-prestressed rebars, while fully cracked referred to after yielding of non-prestressed rebars. Natural axis varies depending on applied moment and prestressing force as shown in Fig.7.

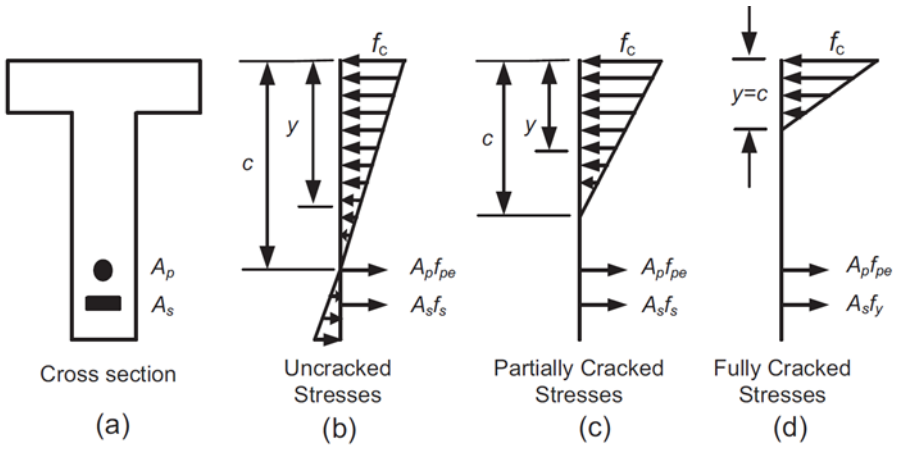

Fig.7. Stress distributions of uncracked, partially cracked and fully cracked UPPC sections

Moment of inertia of fully cracked section is the lower bound of the moment of inertia of partially cracked section. I_{cr} can be obtained as the transformed moment of inertia of the cracked section assuming the amount of reinforcing steel

International Journal of Advances in Engineering and Management (IJAEM)
Volume 3, Issue 2, pp: 108-129www.ijaem.net ISSN: 2395-5252

equivalent to the unbounded prestressing tendons. Equivalent cross-section area:

$$A_{pe} = \frac{A_p f_{pe}}{f_y}$$

Where, A_p : cross sectional area of unbonded tendons; f_{pe} : effective prestress in unbonded tendons, and f_y: yielding stress of non-prestressed steel.

After converting the unbonded prestressing steel to an equivalent of non-prestressing steel using Eq.(2), the neutral axis depth c will coincide with the depth to centroid y at the fully cracked state as shown in Fig.8.

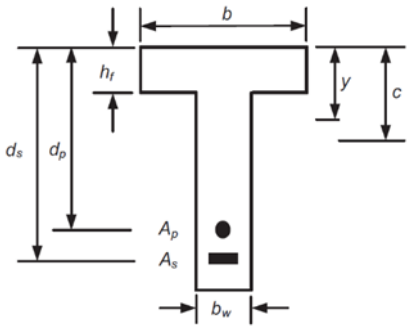

Fig.8. Typical flanged section

According to structural mechanics, it can be defined that:

$$\frac{1}{2}by^2 - \frac{1}{2}(b - b_w)(y - h_f)^2 = n_s A_s(d_s - y) + n_p A_{pe}(d_p - y)$$

Where, $n_s = \frac{E_s}{E_c}$ and $n_s = \frac{E_p}{E_c}$ are the modular ratios for non-prestressed steel and prestressed steel.

The corresponding I_{cr}:

$$I_{cr} = \frac{1}{3}by^3 - \frac{1}{3}(b - b_w)(y - h_f)^3 + n_s A_s(d_s - y)^2 + n_p A_{pe}(d_p - y)^2$$

For rectangular section, $b = b_w$.

Considering two spans UPPC beam with identical spans l with identical point load P at mid-span position, when the applied moment exceeds the corresponding cracking moment M_{cr}, the short-term deflection at mid-span:

$$\delta = \frac{7Pl^3}{768E_c I_e} = \frac{7Ml^2}{120E_c I_e}$$

According to the experiment by Chan [5], 18 two-span continuous beams partially prestressed with external tendon were tested failure. Fig.9 shows the detailed dimension of tested specimens. Two types of tendons (7-wire steel stands of 12.9 mm normal diameter, and Parafil ropes of 10.5 mm normal core diameter made of aramid fiber-reinforced polymer (AFRP)). Two group of tested specimens (wire steel (SCS) and Parafil (PSC)) were tested in the experiment. SCS1-SCS4 and SCS3 were prestressing before testing, while SCS14-SCS15 had been loaded before prestressed. To quantify the amount of flexural reinforcement, reinforcement index was used:

$$\omega = \frac{A_p f_{ps} + A_s f_s - A_s' f_s'}{b d_{ctf} f_c'}$$

Where, A_p : cross-sectional area of prestressing tendons; A_s and A_s' : cross-sectional areas of the bottom and top non-prestressed steel respectively; b: width of the section; d_{ctf}: depth to centroid of tensile force; f_{ps}: tendon stress at peak load; f_s and f_s': tensile stresses of the bottom and top non-prestressed steel at ultimate respectively; f_c': cylinder compressive strength of concrete.

International Journal of Advances in Engineering and Management (IJAEM)
Volume 3, Issue 2, pp: 108-129www.ijaem.net ISSN: 2395-5252

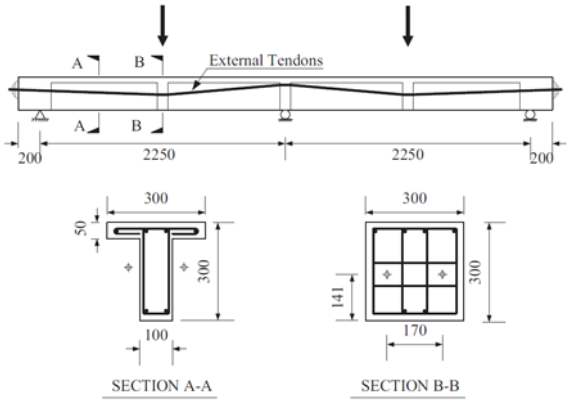

Fig.9. Dimensions of test specimens by Chan at HKU (mm)

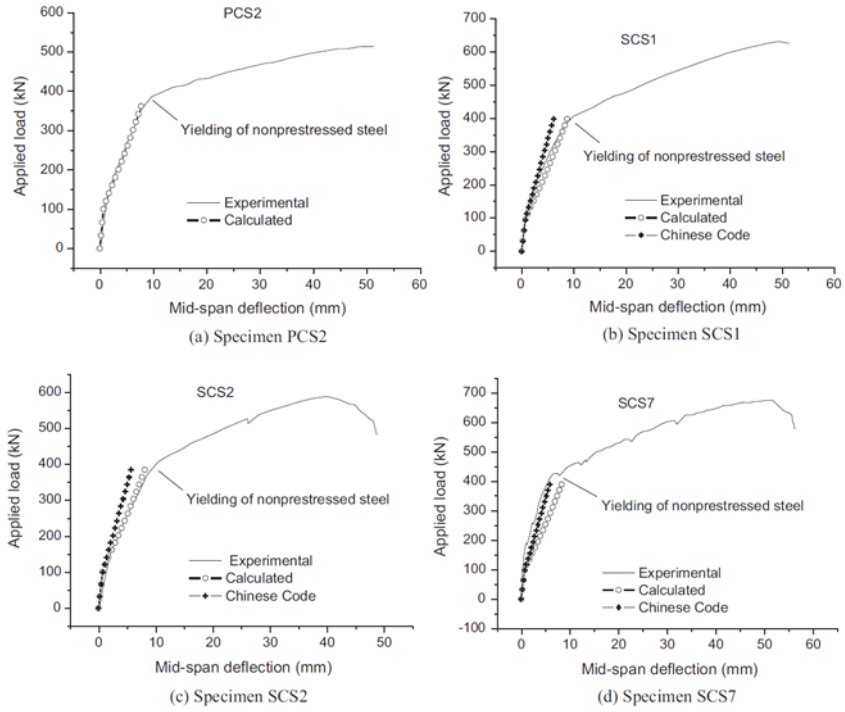

Fig.10. Comparison of prediction results with experimental results by Chan

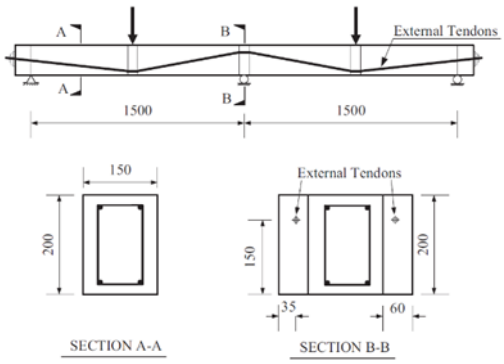

Fig.11. Dimensions of test specimens by Harajli et al. (mm)

International Journal of Advances in Engineering and Management (IJAEM)
Volume 3, Issue 2, pp: 108-129www.ijaem.net ISSN: 2395-5252

Fig.10 shows the load-deflection relationship of the experiments. Comparing the experiment and analysis result, it can be seen the favorable agreement fit the yielding of non-prestressed steel.

According to experimental work by Harajli et al. [6] Seven two-span continuous concrete beams were tested in this experiment. The detailed dimensions of test specimens are shown in Fig.11. Two types of prestressing tendons (wires of 5 mm diameter and 7-wire strands of 8 mm normal diameter) were adopted. Fig.12 shows the load-deflection relationship of the experiment. The result shows the favorable agreement till yielding of non-prestressed steel between the experiment and the analysis result.

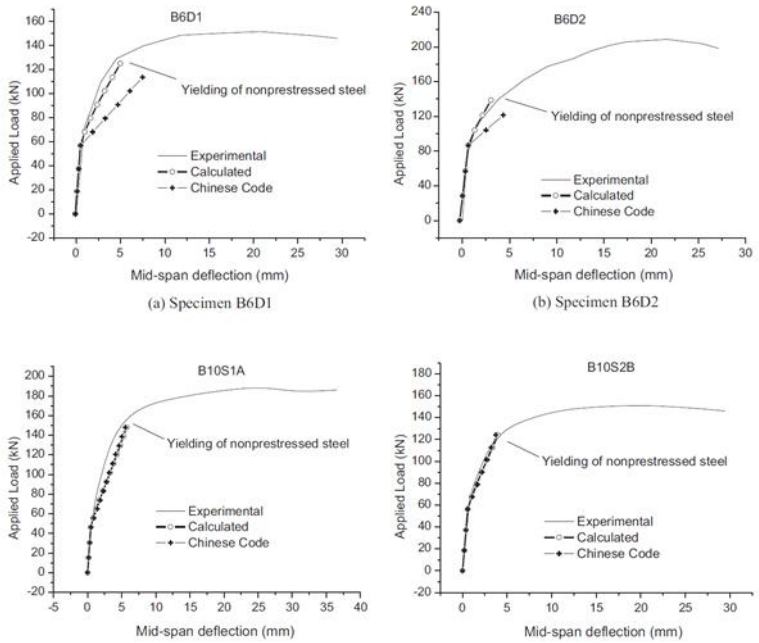

Fig.12. Comparison of prediction results with experimental results by Harajli et al

$\frac{I_e}{I_g}$ and $\frac{M}{M_{cr}}$ were used to investigate variation of effective moment of inertia I_e with applied moment M. Fig.13 shows relationship between $\frac{I_e}{I_g}$ and $\frac{M}{M_{cr}}$. It can be seen that $\frac{I_e}{I_g}$ increased sharply for $\frac{M}{M_{cr}}$ below 2.0, and gradually became stable with increasing of applied moment. The larger the reinforcement index of mid-span is, the larger the value of $\frac{I_e}{I_g}$.

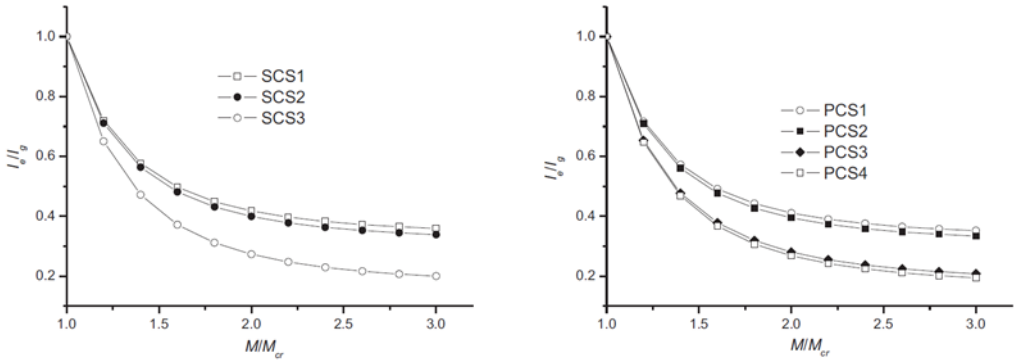

Fig.13. Typical variation of $\frac{I_e}{I_g}$ and $\frac{M}{M_{cr}}$

DESIGN OF PARTICALLY PRESTRESSED CONCRETE BEAMS BASED ON THE CRACKING CONTROL PROVISIONS

According to Karayannis and Chalioris [7], the proposed method first is to estimate the stress of non-prestressed reinforcement based on allowable

International Journal of Advances in Engineering and Management (IJAEM)
Volume 3, Issue 2, pp: 108-129www.ijaem.net ISSN: 2395-5252

crack width as stated in ACI 318 and Eurocode 2. Then, using proposed cubic equation to determine the depth of compression zone. Next, effective pre-strain of the prestressing steel and prestressed force are to be calculated.

Eurocode 2 (EC2-92) recommended how to calculate for characteristic value of design crack width, w_k:

$$w_k = \beta s_{rm} \varepsilon_{rm}$$

Where,

$$\varepsilon_{rm} = \frac{\sigma_s}{E_s}\left[1 - \beta_1\beta_2\left(\frac{\sigma_{sr}}{\sigma_s}\right)^2\right]$$

$$s_{rm} = 50 + 0.25k_1k_2\frac{\phi}{\rho_r}$$

β: coefficient hat equals to 1.7 for load induced cracking and for restraint cracking in sections with a minimum dimension in excess of 800 mm, 1.3 for restraint cracking in sections with a minimum dimension depth, breadth or thickness of 300 mm or less (value for intermediate section sizes may be interpolated),

β_1: coefficient that takes account of the bond properties of the bars (1.0 for high bond bars and 0.5 for plain bars),

β_2: coefficient that takes account of the duration of the loading or of repeated loading (1.0 for a single, short term loading and 0.5 for a sustained load or for many cycles of repeated loading),

k_1: coefficient that takes account of the bond properties of the bars (0.8 for high bond bars and 1.6 for plain bars),

k_2: coefficient that takes account of the form of the strain distribution (0.5 for bending and 1.0 for pure tension),

E_s: design value of modulus of elasticity of reinforcing steel,

σ_s: stress of the tensional reinforcement calculated on the basis of a cracked section,

σ_{sr}: stress of the tensional reinforcement calculated on the basis of a cracked section under the loading conditions causing first cracking that equals to: f_{ctm}/ρ_r,

f_{ctm}: mean value of axial tensile strength of concrete,

ρ_r: effective reinforcement ratio that equals to: $A_s/A_{c,eff}$,

A_s: area of reinforcement contained within the effective tension area,

$A_{c,eff}$: effective tension area that is generally the area of concrete surrounding the tension reinforcement, that equals to:

$$A_{c,eff} = b \cdot \min\left\{\begin{matrix} 2.5(h-d) \\ \frac{(h-x)}{3} \\ \frac{2.5(c+\phi)}{2} \\ \frac{h}{2} \end{matrix}\right\}$$

h, b: overall depth (height) and width of the member, respectively,

d: effective depth of the member,

x: neutral axis depth,

c: clear cover to the longitudinal reinforcement and

ϕ: bar size (for mixture of bar sizes in a section, an average bar size may be used).

According to above equations., the quadratic equation can be obtained:

$$(\beta\rho_r^2)\sigma_s^2 + \left(-\frac{w_k E_s \rho_r^2}{s_{rm}}\right)\sigma_s + (-\beta\beta_1\beta_2 f_{ctm}^2) = 0$$

If the allowable cracked width, w_k, is given, then the value of σ_s can be evaluated.

For the Eurocode 2 (EC2-04), the calculation of crack width was modified based on relationship of, ε_{sm}, average strain of tensional steel, average strain in concrete between cracks, ε_{cm}, and maximum crack spacing $S_{r,max}$:

$$w_k = S_{r,max}(\varepsilon_{sm} - \varepsilon_{cm})$$

Where

$$(\varepsilon_{sm} - \varepsilon_{cm}) = \frac{\sigma_s - k_t\left(\frac{f_{ct,eff}}{\rho_{p,eff}}\right)(1 + \alpha_e\rho_{p,eff})}{E_s}$$

$$\geq 0.6\frac{\sigma_s}{E_s}$$

$$s_{r,max} = k_3c + k_1k_2k_4\frac{\phi}{\rho_{p,eff}}$$

when $k_3 = 3.4, k_4 = 0.425$

$$s_{r,max} = 3.4c + 0.425k_2k_4\frac{\phi}{\rho_{p,eff}}$$

k_t: the factor dependent on the duration of the load (0.6 for short term loading and 0.4 for long term loading),

$$f_{ct,eff} = f_{ctm}$$

$$\rho_{p,eff} = \frac{A_s + \xi_1^2 A_p}{A_{c,eff}}$$

International Journal of Advances in Engineering and Management (IJAEM)
Volume 3, Issue 2, pp: 108-129www.ijaem.net ISSN: 2395-5252

$$A_{c,eff} = b \cdot \min\left\{\begin{array}{l} 2.5(h-d) \\ \dfrac{(h-x)}{3} \\ \dfrac{h}{2} \end{array}\right\}$$

The value of σ_s can be calculated by the following equation:

$$\sigma_s = \frac{w_k E_s}{s_{r,max}} + k_t f_{ctm}\left(\frac{A_{c,eff}}{A_s} + \frac{E_s}{E_{cm}}\right)$$

In ACI 318-95, the calculation of crack width is adopted as following:

$$w = 11.0225 \times 10^{-6} \beta f_s \sqrt[3]{d_c A}$$

Where,

β: ratio of distances to neutral axis from extreme tension fibre and from centroid of reinforcement, approximately equal to 1.2 for beams and 1.35 for slabs,

d_c: distance between edge and centre of the lowest bar (bottom centroid cover),

A: average effective tension concrete area surrounding each reinforcing bar, having same centroid as reinforcement,

f_s : (= σ_s) stress of the tensional reinforcement for the cracked section.

The tensional reinforcement for crack section, σ_s, can be calculated using:

$$\sigma_s = \frac{w_{max} \times 10^6}{11.0225 \beta f_s \sqrt[3]{d_c A}}$$

The major different between Eurocode (EC292 and EC2-04) is that EC2-04 introduce the effective minimum reinforcement ratio. ACI 318-95 can be regarded as the simplification approach compared to Eurocode. Fig.14 shows the relation between tensional stress and effective reinforcement ratio in comparison of between these three design provisions in four typical applications.

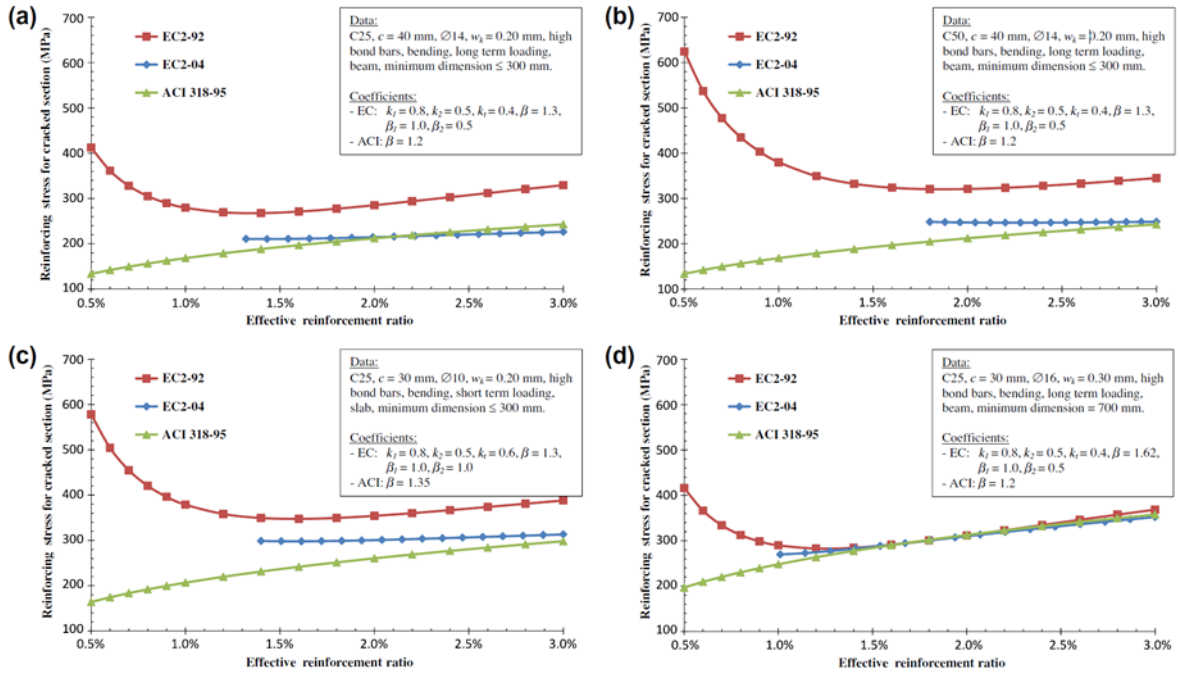

Fig.14. Typical applications of EC2-92, EC2-04 and ACI 318-95 provisions for the crack width control of reinforced concrete members

After obtaining the stress σ_s either from Eurocode or ACI code, then using equilibrium condition of T-section (Fig.15) and mechanics of material, it can be solved for neutral axis depth, x. The cubic equation for neutral axis depth:

$$Ax^3 + Bx^2 + Cx + D = 0$$

where,

$$A = -\frac{b_w}{2}, B = \frac{3b_w d_p}{2}$$

$$C = \frac{3h_f(b_{eff} - b_w)(2d_p - h_f)}{2} - 3a_e(A_{s1}d_{s1} + A_{s2}d_{s2}) + 3a_e d_p(A_{s1} + A_{s2}) + \frac{3a_e M}{\sigma_s}$$

$$D = \frac{3h_f^2(b_{eff} - b_w)(3d_p - 2h_f)}{2} + 3a_e(A_{s1}d_{s1}^2 + A_{s2}d_{s2}^2) - 3a_e d_p(A_{s1}d_{s1} + A_{s2}d_{s2}) - \frac{3a_e M d_{s1}}{\sigma_s}$$

For a simplified case of rectangular beam without compressive reinforcement and $d_{s1} = d_s \cong$

International Journal of Advances in Engineering and Management (IJAEM)
Volume 3, Issue 2, pp: 108-129www.ijaem.net ISSN: 2395-5252

$d_p = d$, then the above coefficients become:

$$A = -\frac{b}{2}, \quad B = \frac{3bd}{2}, \quad C = \frac{3a_eM}{\sigma_s} \quad \text{and} \quad D = -\frac{3a_eMd}{\sigma_s}$$

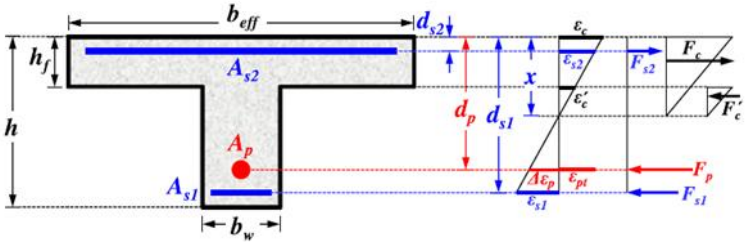

Fig.15. Stain distribution and internal forces across the depth of a T-section cross section

Furthermore, the pre-strain of the prestressed tendons can also be estimated as:

$$\varepsilon_{pt} = \frac{\sigma_s}{A_p E_s (d_{s1} - x)}\left[\frac{b_{eff}x^2 - (b_{eff} - b_w)(x - h_f)^2}{2a_e} + A_{s2}(x - d_{s2}) - A_{s1}(d_{s1} - x) - A_p(d_p - x)\right]$$

For a simplified case of rectangular beam without compressive reinforcement and $d_{s1} = d_s \cong d_p = d$, then the above equation become:

$$\varepsilon_{pt} = \frac{\sigma_s}{A_p E_s}\left[\frac{bx^2}{2a_e(d-x} - (A_s + A_p)\right]$$

$$F_p = \sigma_s\left[\frac{bx^2}{2a_e(d-x)} - A_s\right]$$

The maximum of prestressing reinforcement can be derived as:

$$A_{p,\max} = \frac{\left[\frac{b_{eff}x^2 - (b_{eff} - b_w)(x - h_f)^2}{2a_e} + A_{s2}(x - d_{s2}) - A_{s1}(d_{s1} - x)\right]}{(d_p - x)}$$

Similarly, for a simplified rectangular beam:

$$A_{p,\max} = \frac{bx^2}{2a_e(d-x)} - A_s$$

For the non-prestressed reinforcement, the following equation can be derived:

$$A_{s,\min} = \frac{k_c k f_{ct,eff} A_{ct}}{\sigma_s}$$

Where,

A_{ct}: area of concrete in tension just before the formation of the first crack,

k: coefficient for the effect of non-uniform self-equilibrating stresses, equal to 1.0 for webs with height 6300 mm or flanges with width 6300 mm, 0.65 for webs with height P800 mm or flanges with width 6800 mm and for intermediate values may be interpolated,

k_c: coefficient that takes account the stress distribution within the section immediately prior to cracking and of the change of the lever arm, equal to 1.0 for pure tension and for bending with or without axial force: $= 0.4\left[1 - \frac{\sigma_c}{k_1(\frac{h}{h^*})f_{ct,eff}}\right] \le 1$ for rectangular cross-sections and webs of T-shaped and box sections, where:

$$h^* = \min(h, 1m)$$

$= 0.9\frac{F_{cr}}{A_{ct}f_{ct,eff}} \ge 0.5$ for flanges of T-shaped and box sections,

σ_c: average concrete stress that equals to: $N_{Ed}/(bh)$, where b, h are width and height of the cross-section, and N_{Ed} is the axial force at the serviceability limit state (positive for compression),

k_1: coefficient considering the effects of axial forces on the stress distribution, that equals to 1.5 for compressive and $2h^*$ / $(3h)$ for tensile axial force, and

F_{cr} : absolute value of the tensile force within the flange immediately prior to cracking due to the cracking moment calculated

With $f_{ct,eff}\,(= f_{ctm})$.

PARTIALLY PRESTRESSED CONCRETE

According to Au and Du's research study [8], two type of partially prestressed concrete beams were analyzed; one is bonded partially prestressed concrete (PPC), another one is unbonded partially prestressed concrete.

First, the results investigated by researchers show compared to fully prestressed concrete (FPC) beams, partially prestressed concrete (PPC) beams exhibit larger ultimate deflections, higher ductility, and higher energy absorption. Moreover, the cracks of PPC beams occur in lower load level with higher stiffness after cracking, and the width and spacing of cracks are smaller. In addition, a significant increase in yield curvature and a decrease in curvature ductility can be observed with the decrease in effective prestress.

International Journal of Advances in Engineering and Management (IJAEM)
Volume 3, Issue 2, pp: 108-129www.ijaem.net ISSN: 2395-5252

The main point for the design of fatigue is to determine the stress ranges in prestressed and non-prestressed steel and in concrete, then to make a relation between these ranges to the fatigue strength of respective materials.

Concrete can sustain a fluctuating stress between zero to 50% of its static strength for around 10 million cycles in compression, tension or flexure without failure. Therefore, there is no fatigue failure of concrete in PPC members. For non-prestressed steel, the fatigue of deformed bar is mainly influenced by stress range, bar size, geometry of deformation, bending and welding characteristics. For prestressed steel, the main influence factor on fatigue strength is the stress range, which depends on loading range and prestressing level.

The cracking is allowable for PPC members, but the crack width shall not exceed the maximum crack width limits. There are two approaches to determine the relationship between crack width and strain in the members. The net steel stress approach is based on the net change in steel stress from the decompression moment to the stage at which the crack width is to be determined. The fictitious or nominal concrete method is based on the fictitious concrete tensile stress at the extreme fiber, assuming an uncracked homogeneous section.

In bilinear computation method, gross moment of inertia I_g is used to calculate for the deflection before cracking, and I_{cr} is used to compute for deflection after cracking.

The reinforcement index is main parameter to describe ductility of bonded PPC flexural members, and there is only slightly effect on ductility for partial prestressing ratio.

The behavior of UPPC members is different from bonded PPC members as shown in Fig.16. The effective stress f_{pe} and stress increment Δf_{ps} are the main approach to find the ultimate tendon stress f_{ps} at flexural failure of a beam with unbonded tendons. The influenced factors of stress increments are concrete compressive strength, amount of prestressing tendons, and non-prestressed reinforcement, the span-to-depth ratio. Three categories can be classified in term of ultimate tendon stress methods: those based on regression or lower bound estimates, those based on the concept of Baker's bond reduction coefficient and deformation-based approaches.

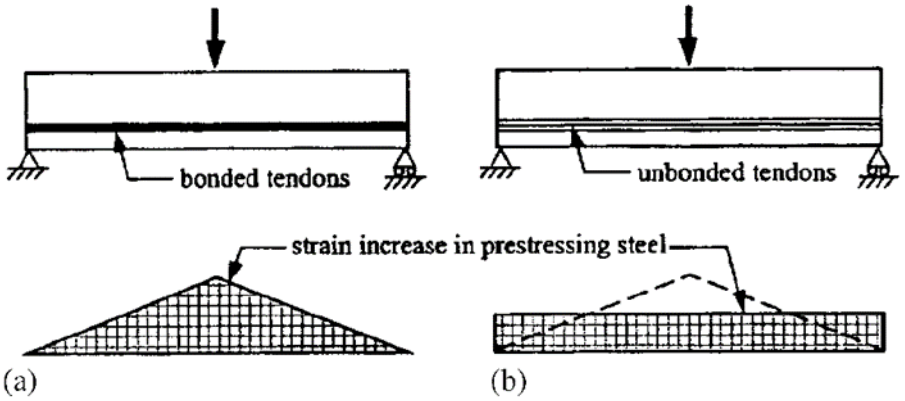

Fig.16. Stain increase in prestressing steel: (a) beam with bonded tendons; (b) beam with unbonded tendons

The ductility of simple span and fully loaded continuous UPPC beam is good compared to bonded post-tensioned beams. The study on reasonable range of amount of prestressing shall be made to ensure the ductility of strengthened members.

BEHAVIOUR OF CORRODED BONDED PARTALLY PRESTRESSED CONCRETE BEAMS

According to the research study of Moawad et al. [9], six beams (150 mm width, 400 mm height and 4500 mm length) simply supported with clear span of 4200 mm were prepared for the experiment as shown in Fig.17. The fabricated of the beams were divided into two stages: casting of six partially prestressed concrete beams and using corrosion technique of four beams. Concrete strengths were 40 MPa and 80 MPa respectively. Four partially prestressed concrete beam were subjected to the electrochemical accelerated corrosion technique. Fig.18 shows the drainage system that keeps the media wet for transporting the electrical filed in the samples. The current intensity was around 10 μ/mm^2 for the specimens.

The beams were subjected to the concentrated load at 700 mm from mid-span using two hydraulic jacks of 800 kN capacity as shown in Fig.3. Linear variable differential transducers,

International Journal of Advances in Engineering and Management (IJAEM)
Volume 3, Issue 2, pp: 108-129www.ijaem.net ISSN: 2395-5252

(LVDT) and electrical strain gauges were used to measure the longitudinal strains of specimens.

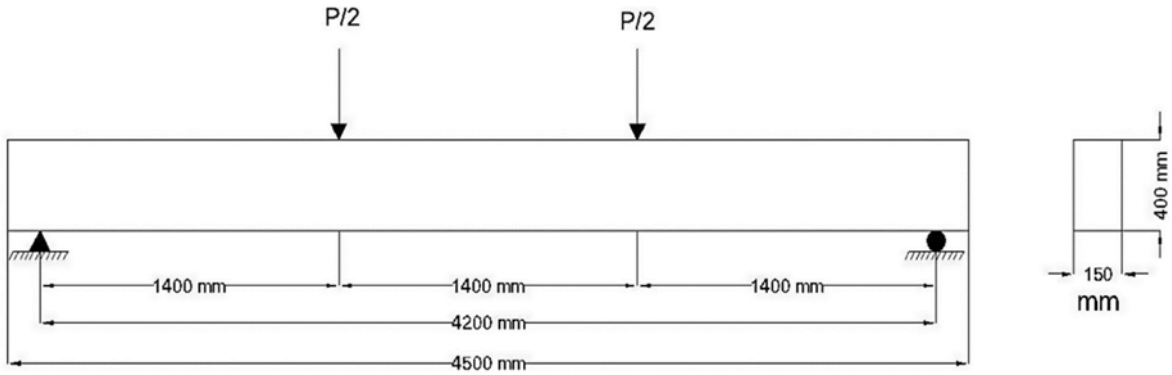

Fig.17. Dimensions of tested beam

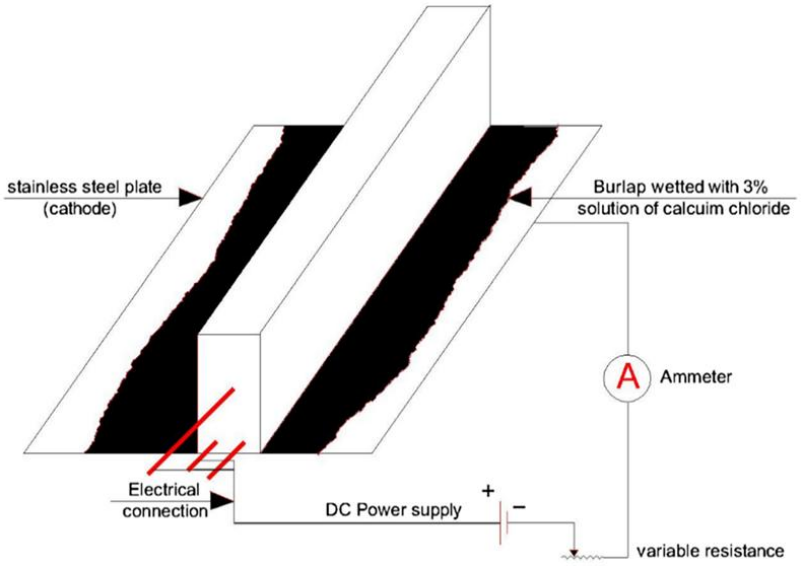

Fig.18. The drainage system that keeps the media wet for transporting the electrical filed in the samples

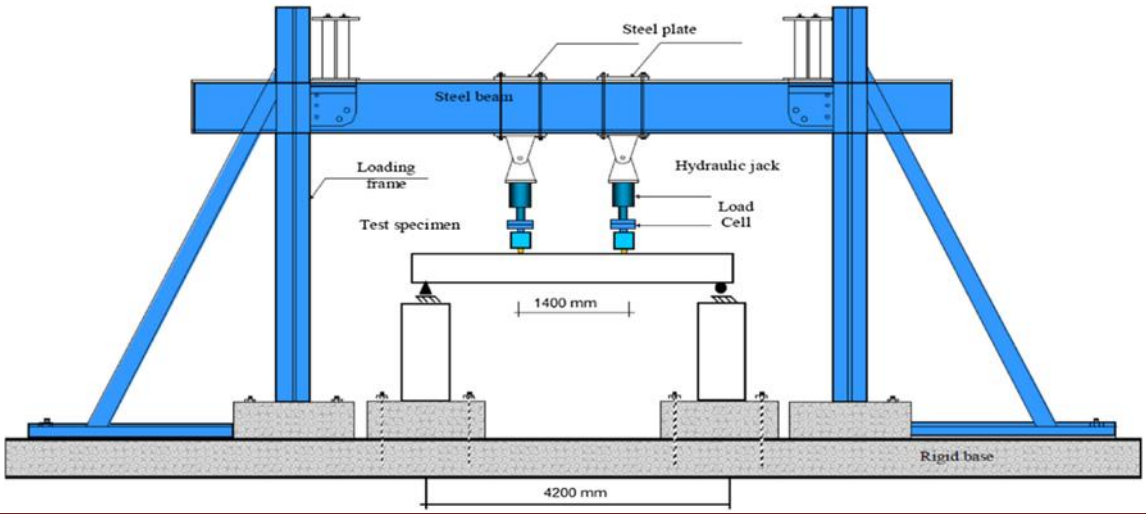

International Journal of Advances in Engineering and Management (IJAEM)
Volume 3, Issue 2, pp: 108-129www.ijaem.net ISSN: 2395-5252

Fig.19. Test setup

For B2 and B5, the non-prestressed steel and prestressed tendon were both exposed to corrosion at the same time with same duration and conditions. It can be seen that the deterioration of prestressed tendon occurred due to complete filling of grout, while the deterioration of non-prestressed steel bars corroded to being exposed to corrosion conditions such as PH level, chemical attack and chloride penetration. Small hairline cracks were observed also at anchorage zone for B2 because of corrosion of anchorage plate. For B3 and B6, only non-prestressed steel was exposed to corrosion at the same time and the same conditions with the same duration. Cracks were observed at bottom and side of the beam. The corroded beam showed the horizontal crack at main longitudinal steel reinforcement, which caused by the accumulation of corrosion products that increased the volume of reinforcement.

Fig.20 shows the failure modes and crack pattern of the specimens. Fig.21 shows the deterioration of the concrete against corroded rebar for samples. The following main observations were made due to Fig.20:

Failure modes of normal compressive strength were more ductile compared with the high strength one.

The crack pattern is distributed along the entire length with small crack width and high number to the grade of concrete.

The crack pattern of 80 MPa specimen in region between two concentrated loads was distributed along the length with larger width and fewer compared to 40Mpa.

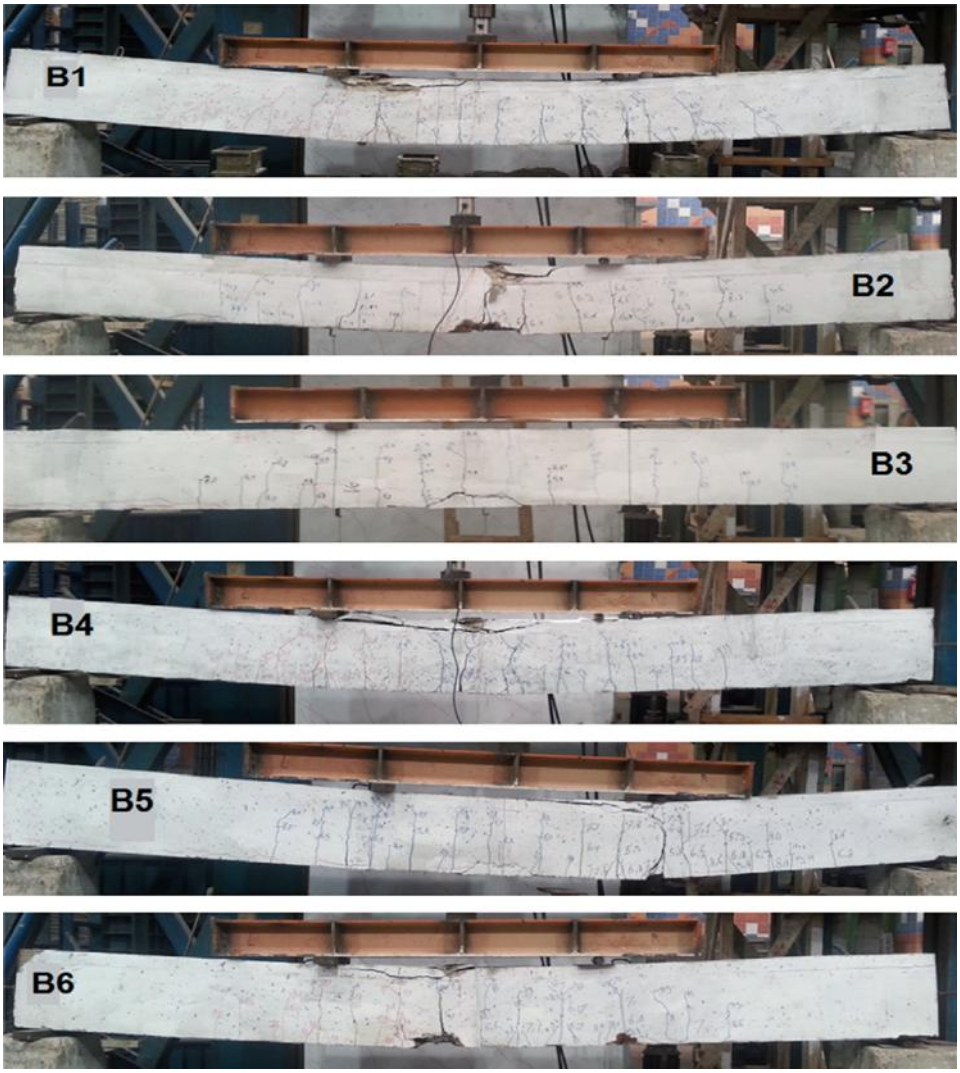

Fig.20. Crack pattern and failure for specimens

International Journal of Advances in Engineering and Management (IJAEM)
Volume 3, Issue 2, pp: 108-129www.ijaem.net ISSN: 2395-5252

Fig.21. Deterioration of the concrete against corroded rebar for sample

Due the experiment results, the flexural capacity, initial stiffness and ductility of beams exposed to corrosion were reduced. These are attributed to the steel corrosion. Higher strength of concrete gave better performance in terms of flexural capacity, initial stiffness and stress crack corrosion. It can be achieved by adding of pozzolanic materials (silica fume, fly ash, etc.) that prevent chloride diffusion. Lower ductility observed for 80 MPa specimen, which may have caused by the brittleness of high strength concrete. For partially and fully corrosion, there were slightly differences between the specimens. This can be attribute to the damage of the bonded prestressed strands against the corrosion not being observed. The anchorages and end stubs shall be fully protected to ensure no corrosion in the tendon.

Analytical study was made for the validation with the above experiment. The stress-strain relationship for the strands is calculated by:

$$f_{ps} = \varepsilon_{ps}\left[A + \frac{B}{\{1 + (C\varepsilon_{ps})^{D}\}^{\frac{1}{D}}}\right] \leq f_{pu}$$

Where

f_p: stress in the steel strand;

ε_{ps}: strain in the steel strand;

f_{pu}: ultimate stress in the steel strand and

$A = 384$, $B = 27616$, $C = 119.7$, and $D = 6.43$ (constants)

The estimation of the minimum area of the corroded rebar (AF) is shown in the following:

a. Compute the mean and the standard deviation for the three areas for which diameters were measured ($R(x)$)

Mean area= $AR = \frac{1}{4} * \sum_{x=1}^{4} R(x)$

Standard deviation:

$$SD = \sqrt{\frac{1}{3} * \sum_{x=1}^{4} (AR - R(x))^2}$$

b. Compute the derived mean and the derived standard deviation. The derived mean:

$$U = AR$$

The derived standard deviation:

$$SM = 1.48 * SD$$

c. Compute the coefficient of variation

Coefficient of variation = $CV = \frac{SM}{U}$

d. Calculate the partial safety factor

Partial safety factor = $SF = (4.5 * CV) + 1$

e. Calculate the characteristic area

Characteristic area = $AK = U - 1.64SM$

f. Finally, calculate the probable minimum area of the corroded rebar

Probable minimum area = $AF = \frac{AK}{SF}$

The prediction and measurement shows a good correlation as shown in Fig.22.

International Journal of Advances in Engineering and Management (IJAEM)
Volume 3, Issue 2, pp: 108-129www.ijaem.net ISSN: 2395-5252

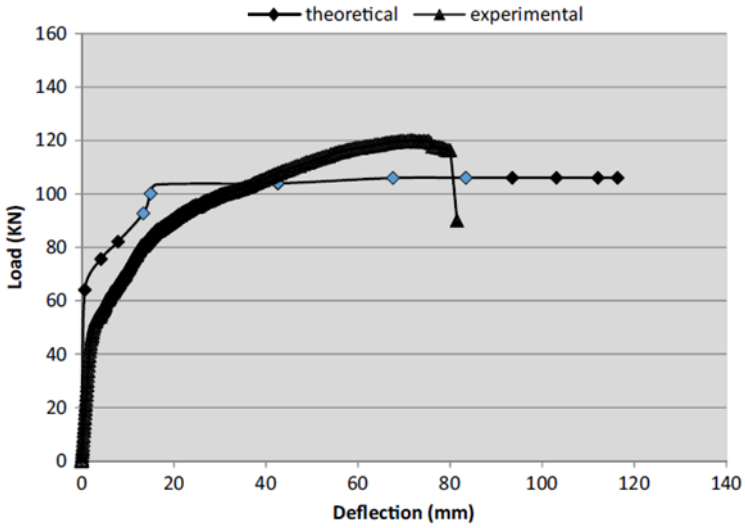

Fig.22. Theorical and experimental result of load-deflection curve for sample B5

CRACK WITH PREDICTIONS OF REINFORCED AND PARTIALLY PRESTRESSED CONCRETE BEAMS: A UNIFIED FORMULA

Chowdhury [10] conducted the study for 12 partially prestressed simply-supported box beams in the experiment. The purpose of the experiment is to observe under static loadings the beams' cracking characteristics in term of spacing and width. Table 1 shows the details of partially prestressed box beams. The beams were loaded symmetrically at two points a certain distance apart. The crack spacings were measured at around 60% to 70% of the ultimate load.

a. Derivation of crack width formula

The crack width might be taken as the difference between elongation of steel and concrete in between two adjacent cracks as following:

$$w_{cr} = \varepsilon_s l_{cr} - \varepsilon_c l_{cr}$$

Where w_{cr} is average crack width, l_{cr} is the average crack spacing, ε_s is the average strain in tensile reinforcement and ε_c is the average tensile strain in concrete at the same level as the reinforcement.

Due to the effects of shrinkage and creep, the elongation of concrete can be ignored. Thus, the above equation becomes:

$$w_{cr} = \varepsilon_s l_{cr} = (f_s/E_s) l_{cr}$$

Due to experiment results (Table 2), the average crack spacing can be derived as following:

$$l_{cr} = 0.6(c - s) + 0.1(\frac{\Phi}{\rho})$$

Where c is the concrete cover, s is the average spacing between the reinforcing bars, Φ is the average bar diameter and ρ is the reinforcement ratio.

Therefore, the average crack width can be derived as:

$$w_{cr} = (f_s/E_s)\left[0.6(c - s) + 0.1(\frac{\Phi}{\rho})\right]$$

Table 1 Details of partially prestressed box beams

Beam number	Prestressing steel		Reinforcing steel		Reinforcement ratio	Degree of Prestressing	Compressive strength of concrete (MPa)	Beam length (m)
	Number of bars	Bar diameter (mm)	Number of bars	Bar diameter				
19	2	5	1 2	12 16	0.00737	0.25	25.9	5.5
20	5	5	4	12	0.00730	0.50	45.8	5.5
21	7	5	2	12	0.00511	0.75	46.4	5.5
22	10	5	1	12	0.00460	1.00	31.0	5.5

International Journal of Advances in Engineering and Management (IJAEM)
Volume 3, Issue 2, pp: 108-129www.ijaem.net ISSN: 2395-5252

23	2	5	1 2	12 16	0.00737	0.25	30.7	6,8
24	5	5	4	12	0.00730	0.50	32.4	6.8
25	7	5	2	12	0.00511	0.75	33.2	6.8
26	7	5	2	12	0.00511	0.75	31.3	6.8
27	2	5	1 2	12 16	0.00737	0.25	28.4	8.0
28	5	5	4	12	0.00730	0.50	39.1	8.0
29	7	5	2	12	0.00511	0.75	34.4	8.0
30	10	5	1	12	0.00460	1.00	27.8	8.0

Table 2 Parameters used development of average crack spacing formula

Beam number	Average bardiameter (mm)	Steel ratio	The ratio (mm)	Average spacing between bars (mm)	Concrete cover (mm)	Average crack spacing (mm)
2	20	0.01154	1733	120	12	131.6
6	20	0.02309	866	48	12	43.7
10	24	0.03348	717	48	12	48.7
11	20	0.01154	1733	120	12	120.0
21	6.6	0.00511	1292	40	27	126.5
23	10.8	0.00737	1465	62	38	126.9
24	8.1	0.00730	1110	38.5	27	118.2
30	5.6	0.00460	1217	40	40	142.0

a. Comparison with test data

The above average crack width is applied to different steel levels to determine the theorical values of the average crack widths. Fig. 23 shows the relationship between measured and theorical values.

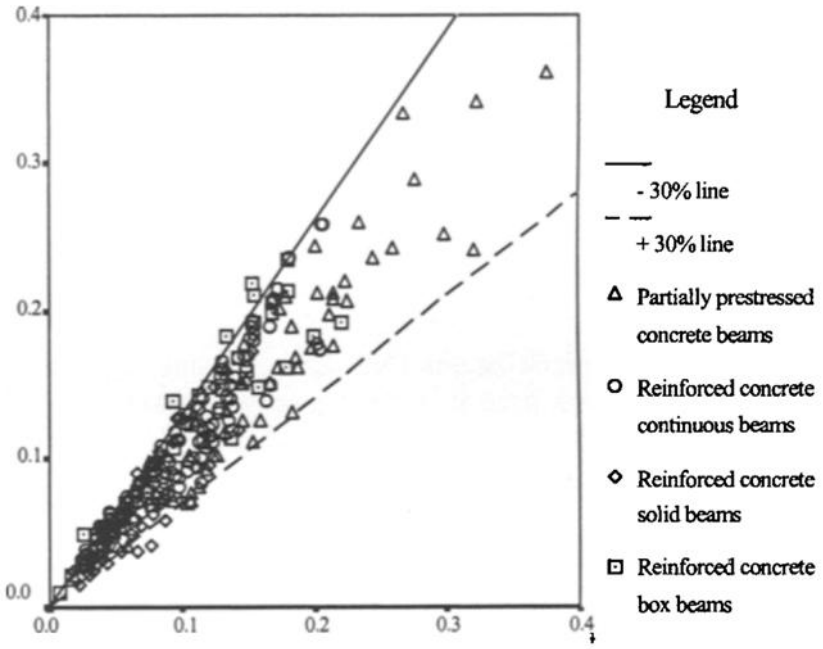

Fig.23. Measured versus calculated crack widths

FLEXURAL STRENGTH PREDICTIONS OF STEEL FIBER REINFORCED HIGH-

International Journal of Advances in Engineering and Management (IJAEM)
Volume 3, Issue 2, pp: 108-129www.ijaem.net ISSN: 2395-5252

STRENGTH CONCRETE IN FULLY/PARTICALLY PRESTRESSED BEAM SPECIMENS

In the study of Padmarajaiah and Ramaswamy [11], eight fully and seven partially prestressed beams were prepared for the experiment. The concrete used in the experiment was the high-strength reinforced concrete (plain concrete strength of 65 MPa).

Two analytical models were proposed for analytical study. Model 1 is based on the modified stress block proposed by Swamy et al. and Hanager and Doherty; model 2 is newly developed of the authors, as shown in Fig.24.

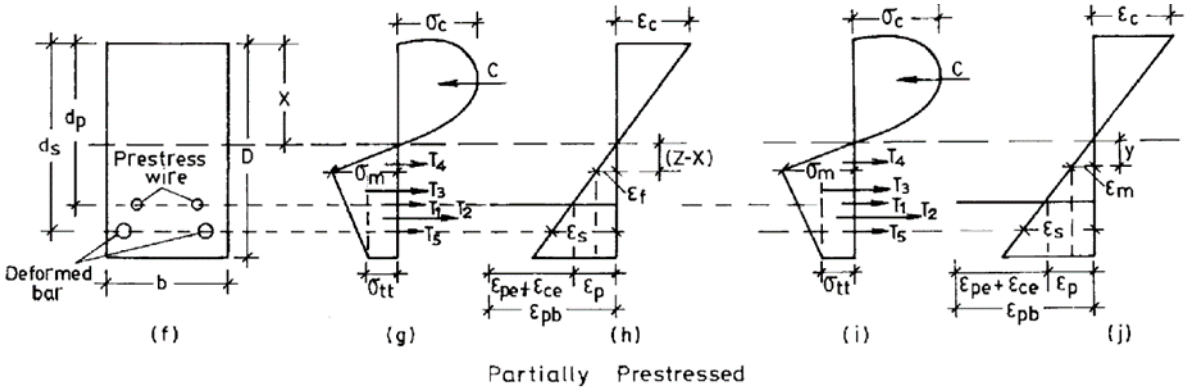

Fig.24. (f) cross-sectional details for partially prestressed beams, (g) and (h) stress and strain diagram for model 1 (i) and (j) stress and strain diagram for model 2

Fig.25 shows the load-deflection curve of specimens, while Fig.26 shows the moment-curvature of specimens, having fiber content of 0%, 0.5%, 1% and 1.5% respectively. It can be seen that by adding the fiber to the partially prestressed beam, both cracking and ultimate flexural strength were enhanced. Fig.27 shows the relationship between ductility factor and fiber reinforcement index. The results show that the toughness and ductility increased with the increase of fiber content.

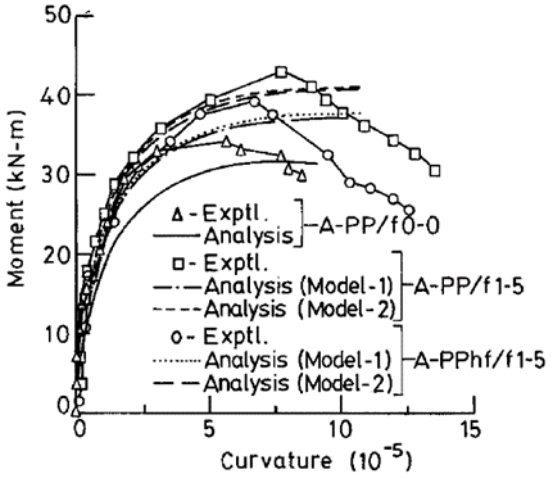

Fig.25 Load-deflection curves

International Journal of Advances in Engineering and Management (IJAEM)
Volume 3, Issue 2, pp: 108-129www.ijaem.net ISSN: 2395-5252

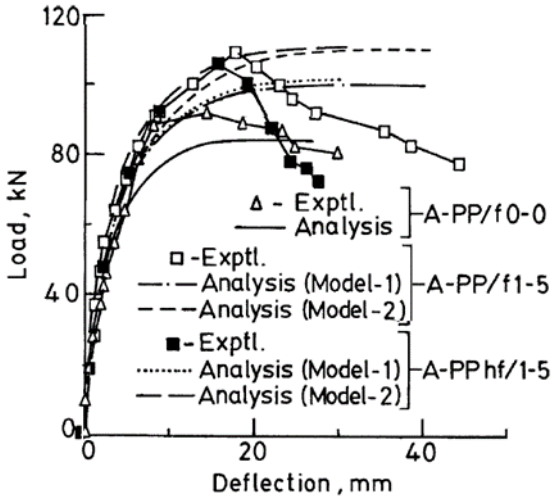

Fig.26. Moment-curvature curves

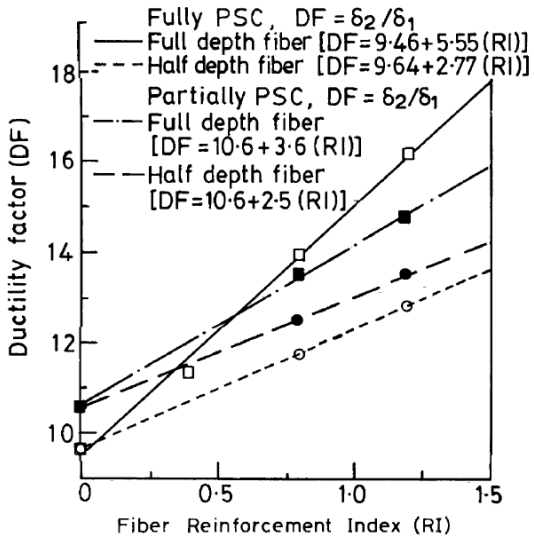

Fig.27. Variation of ductility factor with fiber-reinforcement index

FLEXURAL STRENGTH PREDICTIONS OF STEEL FIBER REINFORCED HIGH-STRENGTH CONCRETE IN FULLY/PARTICALLY PRESTRESSED BEAM SPECIMENS FINITE ELEMENT ANALYSIS OF PARTIALLY PRESTRESSED STEEL FIBER CONCRETE BEAM IN SHEAR

In the research study of Paramasivam et al. [12], finite element of partially prestressed steel fiber concrete was established based on secant modulus approach. The steel fiber concrete was treated as orthotropic material, characterized by appropriate constitutive relations in the principle compressive and tensile directions.

Experimental program of eight T beams (TB21-TB28) were prepared. All the beams were simply supported and subjected to a symmetrical two-point loading. The partial prestressing ratio used in the specimens were 0.0, 0.25, 0.5, and 1.0. The volume fracture of steel fibers varied from 0.0 t0 1.0%.

Due to the results, it can be seen that the finite element formulation can predict the cracking pattern and failure mode of the beams. The first shear cracking load and ultimate load obtained from the finite element analysis were closer compared to the experiment in the beam with higher fiber content and tested at lower shear span (effective depth ratio). The shear strain and the steel strains obtained from the finite element analysis showed good correlation with the experimental results. Due to the results, it can be seen that the addition of steel fibers could improve the behavior of the partially prestressed concrete beams (especially after the appearance of shear cracks). It can increase the

stiffness after the shear cracking and results in enhanced shear strength.

IV. CONCLUSION

It can be concluded that partially prestressed concrete now has been a trend for current researches in structural member such as slab and beam. The practical approach of partially prestressed concrete in slab as vehicle deck of steel truss bridge shows lower cracking load with no crack at service load. In the FRP tendon slab, the result shows that the three parameters: FRP-reduction factor, prestressing level and partial prestressing index, are the main affected factors on the behavior of the slab. The application approaches of partially prestressed concrete in beam are mainly focused on the comparison between theorical prediction and experimental work. For the UPPC continuous beam, the moment inertia of cracked section I_{cr} to calculate for the deflection of the beam with a good agreement to the experiment. The design of the beam section can also be made by using ACI code or Eurocode for the crack allowable crack width and then the prestressing level can be calculated with the proposed method. For the beam exposed to the corrosion, the results show that high strength concrete gave better performance in terms of flexural capacity, initial stiffness and stress crack corrosion, but lower in ductility. Another study has compared the crack width prediction method of beam with the experiment, which shows good validation together. The flexural strength of steel fiber high strength reinforced concrete show higher fiber content give better toughness and ductility. Finally, the finite element analysis of partially prestressed steel fiber concrete beam can well predict the crack pattern and failure mode compared to the experiment.

REFERENCES

[1]. Bruggeling ASG. Partially Prestressed Concrete Structures - A Design Challeng. PCI J.1985;30(2):140–71
[2]. Sutarja IN, Widiarsa IBR. Partial prestressed concrete slabs as an alternative for vehicle decks of steel truss bridges. Procedia Eng. 2015;125: 974–8.
[3]. Wang X, Ali NM, Ding L, Shi J, Wu Z. Static behavior of RC deck slabs partially prestressed with hybrid fiber reinforced polymer tendons. Struct Concr. 2018;19(6):1895–907
[4]. Du JS, Au FTK, Chan EKH, Liu L. Deflection of unbonded partially prestressed concrete continuous beams. Eng Struct. 2016;118: 89–96
[5]. Experimental and numerical studies of concrete beams prestressed with unbonded tendons. University of Hong Kong (Pokfulam Road, Hong Kong); 2008
[6]. Response of externally post-tensioned continuous members. ACI Struct J [Internet]. 2002;99(5). Available from: http://dx.doi.org/10.14359/12307
[7]. Karayannis CG, Chalioris CE. Design of partially prestressed concrete beams based on the cracking control provisions. Eng Struct. 2013;48:402–16
[8]. F.T.K., Au, J.S., Du, Partially prestressed concrete, Structural Analysis and CAD, 2004; 6:127-135
[9]. Moawad M, Mahmoud A, El-karmoty H, El zanaty A. Behavior of corroded bonded partially prestressed concrete beams. HBRC j. 2018;14(1):9–21
[10]. Chowdhury SH. Crack width predictions of reinforced and partially prestressed concrete beams. In: Structural Engineering, Mechanics and Computation. Elsevier; 2001. p. 327–34
[11]. Padmarajaiah SK, Ramaswamy A. Flexural strength predictions of steel fiber reinforced high-strength concrete in fully/partially prestressed beam specimens. Cem Concr Compos. 2004;26(4):275–90
[12]. Paramasivam P, Tan K-H, Murugappan K. Finite element analysis of partially prestressed steel fiber concrete beams in shear. Adv Cem Based Mater. 1995;2(6):231–9